

Dedicated to my Beloved Family

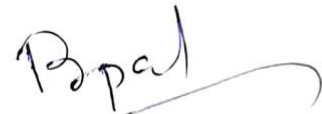
CERTIFICATE

It is certified that the work contained in the thesis titled "***GATE INTERFACE STUDY FOR THE IMPROVEMENT OF ION-CONDUCTING DIELECTRIC BASED LOW OPERATING VOLTAGE THIN FILM TRANSISTOR***" by "***NILA PAL***" has been carried out under my supervision and that this work has not been submitted elsewhere for a degree.

It is further certified that the student has fulfilled all the requirements of Comprehensive, Candidacy, and SOTA for the award of Ph.D. degree.

Date: 20.05.22

Place: Varanasi



Dr. Bhola Nath Pal
(Supervisor)

Dr. Bhola Nath Pal
Associate Professor
School of Materials Science & Technology
IIT (BHU), Varanasi-221005, INDIA

DECLARATION BY THE CANDIDATE

I, **NILA PAL**, certify that the work embodied in this Ph.D. thesis is my own bonafide work carried out by me under the supervision of **Dr. BHOLA NATH PAL** for a period from **December 2017** to **May 2022** at the **SCHOOL OF MATERIALS SCIENCE AND TECHNOLOGY**, Indian Institute of Technology (Banaras Hindu University), Varanasi, India. The matter embodied in this Ph.D. thesis has not been submitted for the award of any other degree/diploma. I declare that I have faithfully acknowledged and credited the research workers wherever their works have been cited in my work in this thesis. I further declare that I have not willfully copied any other's work, paragraphs, text, data, results, *etc.*, reported in journals, books, magazines, reports dissertations, thesis, *etc.*, or available on websites and have not included them in this thesis and have not cited as my own work.


Date: 20.05.2022

Place: Varanasi

Nilal Pal
(Nilal Pal)

CERTIFICATE BY THE SUPERVISOR

This is to certify that the above statement made by the candidate is correct to the best of my knowledge.


Dr. Bhola Nath Pal

Supervisor

Dr. Bhola Nath Pal
Associate Professor
School of Materials Science & Technology
IIT (BHU), Varanasi-221005, INDIA


Dr. Chandana Rath 20/5/2022

Coordinator
समन्वयक

School of Materials Science & Technology/पदार्थ विज्ञान एवं प्रौद्योगिकी स्कूल
Indian Institute of Technology/भारतीय प्रौद्योगिकी संस्थान
(Banaras Hindu University), Varanasi/काशी हिन्दू विश्वविद्यालय, वाराणसी

COPYRIGHT TRANSFER CERTIFICATE

Title of the Thesis: “*GATE INTERFACE STUDY FOR THE IMPROVEMENT OF ION-CONDUCTING DIELECTRIC BASED LOW OPERATING VOLTAGE THIN FILM TRANSISTOR*”

Candidate's Name: Ms. Nila Pal

Copyright Transfer

The undersigned hereby assigns to the Indian Institute of Technology (Banaras Hindu University), Varanasi, all rights under copyright that may exist in and for the above thesis submitted for the award of the *Doctor of Philosophy*.

Date: 20.05.2022

Place: Varanasi

Nila Pal
(Nila Pal)

Note: However, the author may reproduce or authorize others to reproduce materials extracted verbatim from the thesis or derivative of the thesis for the author's personal use, provided that the source and the Institute's copyright notice is indicated.

Acknowledgments

At this moment of retrospection, it gives me immense pleasure to acknowledge the persons who I have met directly or indirectly during the course of my work and stay at IIT (BHU). To express my heartfelt gratitude is not only my moral duty, but I consider it an act of pleasure and humility as well.

*First and foremost, I wish to express my sincere gratitude to my supervisor, **Dr. Bhola Nath Pal**, for his trust, excellent guidance, faithful support and valuable suggestions throughout my Ph.D. work. His constant monitoring and interest in my work will remain a happy memory. His patient and enthusiastic approach to my training cannot be expressed in words and I will always remain thankful to him.*

I would also like to express my sincere thanks to RPEC members Prof. P. Maiti, School of Materials Science & Technology, Institute of Technology (Banaras Hindu University), and Prof. Swapnil Patil, Department of Physics, IIT (BHU), for their stimulating help and criticism which incited me to widen my research from various perspectives. I would like to thank the coordinator of the School of Materials Science and Technology, IIT (BHU) for providing different instrumental facilities. I would like to express my sincere gratitude to Dr. Nikhil Kumar (DPGC convener) for his valuable input, suggestions and affectionate attitude.

I wish to express deep regards to all the teachers of the Department Prof. D. Pandey, Prof. R. Prakash, Prof. P. Maiti, Dr. C. Rath, Dr. A. K. Singh, Dr. C. Upadhyay, Dr. A. K. Mishra, Dr. S. K. Mishra, Dr. S. R. Singh, Prof. Jitendra Kumar, Dr. Ashish Singh, Dr. Nikhil Kumar and other for their kind support at all moment during the progress of my research. Also, I am grateful to Dr. Monalisa Pal, Department of Chemistry (BHU) for her support and guidance. I am thankful Dr. Pradip K. Roy, Department of Ceramic Engineering, and Prof. Sandip Chatterjee, Department of Physics, IIT (BHU) for providing lab and instrumental facilities, valuable suggestions and affectionate attitude.

With a deep sense of gratitude, I express my sincere thanks to CIFC, IIT (BHU), Varanasi for their help in carrying characterization of the synthesized samples. I am also grateful to all office staff of the school and authorities of IIT (BHU) for their kind help during my stay to complete the thesis work.

With a special thanks to my pioneer lab mates Dr. Anand Sharma, Dr. Satya Veer Singh, Dr. Nitesh K. Chourasia, and currently Mr. Vishwas Acharya, Mr. Utkarsh Pandey, Mr. Sobhan Hazra, Mr. Rajarshi Chakraborti, Mr. Sandeep, Mr. Pijush kanti Aich, Mr. Akhilesh K. Yadav, Mr. Subarna Pramanik, Ms. Swati Suman and Ms. Shipra Gupta for their suggestion and healthy discussion of my research issues. I am incredibly thankful to my seniors and friends, Dr. Priyanka Tiwari, Dr. Aprna Shukla, Dr. B. Bharati, Dr. Piyali Maiti, Mr. Ravi Prakash, and Mr. Pawan K. Ojha for their support, cooperation and sincere help in many ways and for making my stay here enjoyable and for their time to time encouragement during my bad situations.

It fills me with a deep sense of reverence when I think about my family. Their constant encouragement, moral support, and cooperation at every step of my life can't be expressed in words. I am thankful for their love and blessings. Also, I am grateful to my friends Dr. Subrata Jana, Mr. Arunava Kar, Mr. Suman Bhuiya, and Mr. Ashok Mandal, Ms. Nupur Patra, Ms. Florida Sultana and Afroza Akhtary for their unconditional love and support.

Finally, I bow with reverence and gratitude to thank the Almighty MAHADEV, who has enriched me with such an excellent opportunity and infused the power in my mind to fulfill the work assigned to me.

Date: 20.05.2022

Place: Varanasi

Nila Pal
(Nila Pal)

Contents

<i>Acknowledgements</i>	xi
<i>Contents</i>	xiii
<i>List of Figures</i>	xvii
<i>List of Tables</i>	xxiii
<i>Abbreviations</i>	xxv
<i>PREFACE</i>	xxvii
Chapter 1: Introduction	1
1.1 Background of thin film transistor (TFT) research.....	2
1.2 Brief History and Principles of TFTs.....	4
1.2.1 Field-Effect Mobility (μ).....	8
1.2.2 ON/OFF ratio.....	9
1.2.3 Threshold Voltage (V_T).....	9
1.2.4 Subthreshold Swing (SS).....	10
1.3 TFT Components: Their Role in TFT Characteristics and Material Selection Procedure for Components.....	10
1.3.1 Gate Insulator (Dielectric).....	10
1.3.2 Semiconductor.....	13
1.3.3 Electrodes.....	15
1.4 Requirement of high- κ dielectric in TFT community: Their advantages and drawbacks.....	16
1.5 Role of Interfacial engineering in the improvement of TFT Device performance..	19
1.6 Ferroelectric Field Effect Transistor (FEFET) with ionic ferroelectric gate dielectric.....	22

1.6.1	Retention Time.....	23
1.6.2	Remnant Polarization.....	23
1.7	Scope and Objective of the Present Work.....	24
Chapter : 2 Experimental Part: Materials Synthesis & Characterization, Device		
	Fabrication.....	29
2.1	Materials synthesis.....	30
2.1.1	Synthesis of Li-Al ₂ O ₃ ion-conducting gate-dielectric precursor solution....	31
2.1.2	Synthesis of TiO ₂ and Mn ₂ O ₃ precursor solution.....	31
2.1.3	Synthesis of SnO ₂ precursor solution.....	32
2.1.4	Synthesis of ferroelectric LiNbO ₃ precursor solution.....	32
2.1.5	Synthesis of a-C precursor solution.....	32
2.2.	Device fabrication.....	33
2.2.1	Substrate cleaning.....	33
2.2.2	Device fabrication with a single dielectric layer.....	35
2.2.2.1	SnO ₂ TFT with Li-Al ₂ O ₃ gate-dielectric.....	35
2.2.2.2	SnO ₂ TFT with LiNbO ₃ gate-dielectric.....	35
2.2.3	Device fabrication with bilayer dielectric stack.....	36
2.2.3.1	SnO ₂ TFT with bilayer TiO ₂ /Li-Al ₂ O ₃ dielectric.....	36
2.2.3.2	SnO ₂ TFT with bilayer Mn ₂ O ₃ /Li-Al ₂ O ₃ dielectric.....	37
2.2.3.3	SnO ₂ TFT with multilayer Li-Al ₂ O ₃ /LiNbO ₃ /Li-Al ₂ O ₃ dielectric.....	38
2.2.3.4	SnO ₂ TFT with bilayer Li-Al ₂ O ₃ /a-C dielectric.....	39
2.3	Material characterization and Electrical characterization.....	39
2.3.1	X-ray diffraction.....	39
2.2.2	UV-visible spectroscopy.....	40
2.3.3	Atomic force microscopy.....	40

2.3.4	X-ray photoelectron spectroscopy.....	41
2.3.5	Scanning electron microscopy.....	41
2.3.6	Current measurement.....	42
2.3.7	Capacitance vs. frequency measurement.....	42
2.3.8	Polarization vs. Electric field measurement.....	43
2.3.9	Thin-film transistor characterization.....	43
Chapter 3: Solution-processed Low Voltage Metal-Oxide Transistor by using TiO ₂ /Li-Al ₂ O ₃ stacked Gate Dielectric.....		
		45
3.1	Introduction.....	46
3.2	Results and discussions.....	48
3.2.1	Grazing Incidence X-ray Diffraction pattern of Thin Films.....	48
3.3.2	Surface Morphologies of Thin Films.....	49
3.2.3	Dielectric and Electrical characterization.....	50
3.2.4	Electrical Characterization of Single and Bilayer Thin Film Transistor.....	52
3.3	Conclusions.....	57
Chapter 4: Gate Interface Engineering for Sub-volt Metal-Oxide Transistor Fabrication by Using Ion-conducting Dielectric with Mn ₂ O ₃ Gate Interface.....		
		59
4.1	Introduction.....	60
4.2	Results and discussions.....	62
4.2.1	Powder XRD and GIXRD characterization of Mn ₂ O ₃	62
4.2.2	X-ray photoemission spectroscopy (XPS) of Mn ₂ O ₃	63
4.2.3	UV-Vis absorption studies of thin films.....	64
4.2.4	Surface morphologies of different thin films.....	66
4.2.5	Cross-sectional SEM of TFT device.....	68
4.2.6	Variation of capacitance with frequency and current density with applied field (or voltage) of different dielectric films.....	68

4.2.7	TFT device characterization.....	71
4.3	Conclusions.....	76
Chapter 5: Solution processed Li-Al ₂ O ₃ /LiNbO ₃ /Li-Al ₂ O ₃ Stacked Gate Dielectric for a Low Operating Voltage Ferroelectric Thin Film Transistor.....		
		79
5.1	Introduction.....	80
5.2	Results and discussions.....	82
5.2.1	XRD Analysis	82
5.2.2	UV-Vis Spectra Study.....	84
5.2.3	Surface Morphology.....	85
5.2.4	Dielectric Properties.....	86
5.2.5	Electronic characteristics of Transistors.....	90
5.2.6	Retention Time.....	95
5.3	Conclusions	99
Chapter 6: Application of Microwave Synthesized Ultra-smooth a-C Thin Film for the Reduction of Dielectric/Semiconductor Interface Trap States of an Oxide TFT.....		
		101
6.1	Introduction.....	102
6.2	Results and discussions.....	104
6.2.1	Surface Morphology and Chemical State Study.....	104
6.2.2	Dielectric and Electronic Characterization of MIM Devices.....	107
6.2.3	Electronic Measurements of TFTs.....	109
6.3	Conclusions.....	114
Chapter 7: Conclusions and Future perspectives.....		
		115
7.1	Conclusions.....	116
7.2	Future perspectives.....	119
References		121
List of Publications		147

List of Figures

Figure 1.1 Various applications of metal oxide-based TFTs. Reproduced with permission.[34-40]. Copyright 2019, 2021, 2022 American Chemical Society. 5

Figure 1.2 Schematics of a) main components of thin film transistor and its working principle, and b) various possible TFT device configurations according to the position of electrodes. 6

Figure 1.3 Typical a) I_D vs. V_D and b) I_D vs. V_G characteristics of n-channel transistors.[41] 8

Figure 1.4 Graphical representation of metal-insulator-insulator (MIM) device a) without, and b) with applied bias. Working of a dielectric inserted parallel plate capacitor c) random orientation of the dipoles in without bias condition, and d) directional orientation in applied bias condition. 12

Figure 1.5 a) Capacitance dispersion relation of typical high and low κ dielectric materials, and b) dependence of gate dielectric leakage current with applied field.[41] 13

Figure 1.6 a) The decrease of bandgap values with increasing dielectric constants of well known metal-oxide dielectrics, b) band offset criteria for high- κ dielectrics, where V_e and V_h denote the potential barriers for electron and hole, and CB and VB represent the conduction and valence bands for the semiconducting channel and dielectric films, respectively.[41] 17

Figure 1.7 a) Representation of SBA crystal structure, where blue symbolizes the mobile sodium ion and red and yellow represent oxygen and aluminum atoms, respectively. b) Output and c) transfer characteristics of SBA based Zinc Tin Oxide TFT with varying operating voltage (inset of c) shows the schematic diagram of TFT device).[73] 19

Figure 1.8 Improvement of device performances using different interfacial engineering. Examples of interfacial engineering using a) dielectric stacks, b) self-assembled monolayer (SAM) passivation layer, c) electron-donating gate dielectric/gate electrode interface, and d)

semiconducting bilayer. Reproduced with permission.[77, 81, 83, 84] Copyright 2011,2016,2018,2020 American Chemical Society. 21

Figure 1.9 *Schematic representations of FET and FEFET.....23*

Figure 2.1 *a) Substrate cleaning steps of both types of substrates with standard RCA cleaning method following oxygen plasma treatment, and b) device fabrication steps of a single dielectric layer and the different interfacial layers containing dielectric stack-based thin-film-transistor device.....34*

Figure 2.2 *Metal insulator metal device configurations for dielectric characterizations.....43*

Figure 2.3 *Schematic representation of thin-film-transistor device configuration.....44*

Figure 3.1 *Schematic diagrams of TFT devices, a) device-1 with single layer Li-Al₂O₃ gate-dielectric, b) device-2 with bilayer TiO₂/Li-Al₂O₃ gate-dielectric. MIM devices with c) Li-Al₂O₃ gate-dielectric and, d) TiO₂/Li-Al₂O₃ gate-dielectric.....48*

Figure 3.2 *The GIXRD patterns of a) TiO₂, b) Li-Al₂O₃ dielectric, and c) SnO₂ semiconductor layer annealed at 500°C.....49*

Figure 3.3 *2D AFM images of a) Li-Al₂O₃ and b) TiO₂/Li-Al₂O₃ dielectric. 3D AFM images of e) Li-Al₂O₃ and f) TiO₂/Li-Al₂O₃ dielectric. 2D AFM image of SnO₂ thin film on c) Li-Al₂O₃ and d) TiO₂/Li-Al₂O₃ dielectric. 3D AFM image of SnO₂ thin film on g) Li-Al₂O₃ and h) TiO₂/Li-Al₂O₃ dielectric.....50*

Figure 3.4 *Variation of a) areal capacitance with frequency current density with applied voltage, and b) current density with applied voltage for p⁺⁺-Si/Li-Al₂O₃/Al and p⁺⁺-Si/TiO₂/Li-Al₂O₃/Al MIM devices.....51*

Figure 3.5 Transistor characterizations of single layer and bilayer gate-dielectric SnO₂ TFT. a) and b) output characteristics; c) and d) transfer characteristics; e) and d) linear fit of log (I_D) vs. V_G curve to extract SS value; g) and h) linear fit of (I_D)^{1/2} vs. V_G to extract carrier mobility of device-1 and device-2, respectively.....53

Figure 3.6 Metal-Insulator-Semiconductor structures illustrating the mechanism of variation in transistor performances with single layer and bilayer dielectric stack. Energy band diagram of a) and c) without applied bias, and b) and d) with applied positive bias of device-2 with bilayer TiO₂/Li-Al₂O₃ dielectric and device-1 with single layer Li-Al₂O₃ dielectric, respectively.....56

Figure 4.1 Schematic diagram of the device structures of a) device-1 (without Mn₂O₃ gate interface), b) device-2 (with Mn₂O₃ gate interface), c) MIM device without Mn₂O₃, d) MIM device with Mn₂O₃.....62

Figure 4.2 a) XRD patterns of Mn₂O₃ powder sample, and b) GIXRD patterns of Mn₂O₃ thin film annealed at 550°C.....63

Figure 4.3 XPS spectra of the different elements present in Mn₂O₃ thin film a) survey scan b) Mn 3s and c) Mn 2p states and d) O 1s allocated to Mn-O-Mn (~ 529.81 eV) and Mn-O-H (~ 531.58 eV) of Mn₂O₃ thin film sample annealed at 550°C.....65

Figure 4.4 Optical absorption and transmittance spectra of the solution-processed a) Mn₂O₃ and b) Li-Al₂O₃ thin films annealed at 550°C and 500°C respectively. Tauc plot ((αhv)² vs. hv) of c) Mn₂O₃ and d) Li-Al₂O₃ show direct allowed transition with optical band gap 3.36 eV and 5.70 eV, respectively.....66

Figure 4.5 Two dimensional AFM images of a) Mn_2O_3 , b) $Li-Al_2O_3$, and c) $Mn_2O_3/Li-Al_2O_3$ thin film on ITO. Three dimensional AFM images of d) Mn_2O_3 ($R_{rms} \sim 0.56$ nm), e) $Li-Al_2O_3$ ($R_{rms} \sim 0.28$ nm), and f) $Mn_2O_3/Li-Al_2O_3$ ($R_{rms} \sim 0.74$ nm) thin film on ITO.....67

Figure 4.6 Cross-sectional SEM image of device-2 with a device structure of ITO/ $Mn_2O_3/Li-Al_2O_3/SnO_2/Al$68

Figure 4.7 Variation of a) capacitance vs. frequency, b) current density vs. the applied field, c) current density vs. applied voltage, of $Li-Al_2O_3$ and $Mn_2O_3/Li-Al_2O_3$ gate dielectric with MIM device architecture.....70

Figure 4.8 Typical a) output c), transfer characteristics of device-1 and b) output and d) transfer characteristics of device-2. Linear fit of $(I_D)^{1/2}$ vs. V_G plot for e) device-1 and f) device-2 to extract the slope for charge carrier mobility calculation. Log (I_D) vs. V_G plot for g) device-1 and h) device-2 to determine the slope for subthreshold swing (SS) calculation.....74

Figure 4.9 Energy band diagram of the $Mn_2O_3/Li-Al_2O_3$ dielectric film a) under zero and b) positive gate bias. Energy band diagram of $Li-Al_2O_3$ dielectric film c) under zero gate bias d) under positive gate bias.....76

Figure 5.1 Schematic configuration of SnO_2 FEFET with a) only $LiNbO_3$ (LN) ferroelectric and b) $Li-Al_2O_3/LiNbO_3/Li-Al_2O_3$ (LA/LN/LA) stack dielectric layer as the gate material. Metal-insulator-metal (MIM) devices have been illustrated with c) only ferroelectric and d) stacked dielectric layer, respectively.....82

Figure 5.2 GIXRD patterns of LiNbO₃ thin film a) annealed at 400°C for 1 hour, b) annealed at 500°C for 30 minutes.....83

Figure 5.3 The a) UV-Vis Spectra of LiNbO₃ thin film deposited on quartz glass, b) Taucs plot using the absorbance data to obtain optical band gap of LiNbO₃ thin film annealed at 400°C.....85

Figure 5.4 Surface topography of p⁺⁺-Si/LN a) 2D and, b) 3D; p⁺⁺-Si/LA/LN/LA/Al c) 2D and, d) 3D; p⁺⁺-Si/LN/SnO₂ e) 2D and, f) 3D; p⁺⁺-Si/LA/LN/LA/SnO₂ g) 2D and h) 3D, respectively.....87

Figure 5.5 a) Capacitance dispersion relation with frequency and b) leakage current density vs. voltage measurement; polarization vs. applied field measurement of c) p⁺⁺-Si/LN/Al and d) p⁺⁺-Si/LA/LN/LA/Al MIM device, respectively.....89

Figure 5.6 Output (I_D - V_D) characteristics of an n-channel SnO₂ TFTs with a) LN and c) LA/LN/LA stacked dielectrics, having devices' channel width to length ratio (W/L) =118. Transfer characteristics (I_D - V_G) of the TFT devices with b) LN and d) LA/LN/LA stacked dielectrics, respectively, measured at constant $V_D = 1$ V. Linear fit of $\log(I_D)$ vs. V_G curves at lower V_G region of TFTs with e) LN and, g) LA/LN/LA stacked dielectric for SS value calculation. Linear fit of $(I_D)^{1/2}$ vs. V_G curves of devices with f) LN and, h) LA/LN/LA stacked dielectric, respectively for carrier mobility calculation.....91

Figure 5.7 Transfer characteristics of both devices with different gate voltage range keeping constant drain voltage at 1 V. Gate voltage range -1.5 V to various volts for a) LN, d) LA/LN/LA based TFTs; -1.5 V to 5 V b) LN, e) LA/LN/LA based TFTs; -1.5 V to 10 V for c) LN, f) LA/LN/LA based TFTs, respectively.....94

Figure 5.8 Retention characteristics of FEFET with LA/LN/LA stacked dielectric, measured by keeping $V_G = 0V$ and $V_D = 1V$ with time range a) device-2 and c) device-1 for 10 minutes and b)

device-2 and d) device-1 for 2 hours . The gate voltage of 7 V and -2 V are applied to achieve the ON and OFF states, respectively.....96

Figure 5.9 Schematic configuration of Energy Band diagrams for a) p^{++} -Si/LiNbO₃/SnO₂ and b) p^{++} -Si/Li-Al₂O₃/LiNbO₃/Li-Al₂O₃/SnO₂ at positive applied gate voltage.....98

Figure 6.1 Surface microstructures of bare Li-Al₂O₃ dielectric a) 2D, b) 3D on the top of p^{++} -Si substrates; and b) 2D, d) 3D micrographs after a-C layer passivation.....105

Figure 6.2 XPS spectra of a) Sn 3d from SnO₂ with (red color online) and without (green color online) underlying a-C layer; b) N 1s from a-C with (red color online) and without (navy blue color online) adjacent SnO₂ layer at high resolution.....106

Figure 6.3 Schematic diagrams of metal-insulator-metal (MIM) device structures with a) only Li-Al₂O₃, b) a-C passivated Li-Al₂O₃, c) areal capacitance vs. frequency, and d) current density vs. voltage relationship of both MIM devices.....108

Figure 6.4 Representative device configuration of TFTs a) without (device-1), d) with (device-2) a-C layer. Output characteristics of c) device-1 and e) device-2. Transfer characteristics of d) device-1 and f) device-2 at constant $V_D=1$ V. Linear fitting at lower region of $\log(I_D)$ vs. V_G curves of g) device-1, i) device-2 for Subthreshold Swing value calculation. Linear fitting of $(I_D)^{1/2}$ vs. V_G curve of h) device-1, and j) device-2 to extract the slope for mobility calculation....111

Figure 6.5 The to and fro sweep of gate voltage at constant $V_D = 1$ V for a) device-1 and b) device-2 to check the hysteresis nature of the devices. Cyclic stability test of c) device-1 and d) device-2 with 50 sweep cycles.....113

List of Tables

<i>Table 3.1</i> Summary of the TFT parameters of SnO ₂ transistors with single layer and bilayer stack gate-dielectrics.....	55
<i>Table 4.1</i> Current densities, areal capacitance, and dielectric constants of dielectric films.....	70
<i>Table 4.2</i> Key parameters of SnO ₂ TFTs with and without Mn ₂ O ₃ gate interface.....	73
<i>Table 5.1</i> Summary of the MIM device parameters.....	89
<i>Table 5.2</i> Summary of the TFT parameters.....	93
<i>Table 6.1</i> Summary of key parameters extracted from MIM devices.....	109
<i>Table 6.2</i> Summary of the TFT parameters.....	112

Abbreviations

MO	Metal oxides
BG/TC	Bottom gate/Top contact
SBA	Sodium- β -Alumina
κ	Dielectric constant
AOS	Amorphous oxide semiconductor
TFT	Thin film transistor
LET	Light-emitting transistor
MIM	Metal insulator metal
MFM	Metal ferroelectric metal
FEFET	Ferroelectric field effect transistor
ICMO	Ion conducting metal oxide
XRD	X-ray diffraction
GIXRD	Grazing incidence X-ray diffraction
AFM	Atomic force microscopy
CBM	Conduction band minima
VBM	Valence band minima
RMS	Root-mean-square
SEM	Scanning electron microscopy
UV	Ultraviolet
I-V	Current vs. voltage

C-f	Capacitance vs. frequency
AMLED	Active-matrix light-emitting diode
LA	Li-Al ₂ O ₃
LN	LiNbO ₃
p ⁺⁺ -Si	Heavily doped silicon
ITO	Indium Tin Oxide
IZO	Indium Zinc Oxide
C	Areal capacitance
d	Thickness of dielectric
I _D	Drain current
I _G	Gate current
V _D	Drain voltage
W/L	Channel width to length ratio
V _G	Gate voltage
V _T	Threshold voltage
SS	Subthreshold swing
μ	Field-effect mobility
E _g	Band gap
h	Planck's constant
N _{SS} ^{Max}	Interfaces states
q	Electronic charge

PREFACE

Thin-film transistors (TFT) serve as the foundation of flat-panel display devices. In order to achieve great performance while lowering production costs, researchers looked into a variety of materials in TFTs. Metal-oxides have gained a lot of attention in recent years for thin film transistors due to their broad area manufacturing compatibility, high mobility, and low leakage density properties. At present time, higher resolution, larger screen sizes, and reduced power consumption in FPDs have become increasingly important, which pushes traditional amorphous Si (a-Si) TFT technology to its limits. On the other hand, metal-oxide TFTs have been widely explored for a variety of applications, including phototransistor arrays, gas and pressure sensors, light emitting transistors, photo-detectors, memory, and synaptic devices etc. These metal oxide TFTs possess excellent temperature and chemical robustness, as well as superior mobility and a significant ON/OFF ratio, all of which are crucial for practical applications. However, because of the low dielectric constant (κ) of traditional SiO_2 gate dielectric, most of these TFTs require a fairly high voltage level (<40 V), limiting their utility in portable electronic gadgets (e.g., laptop, tablet, mobile, etc.). Furthermore, the high- κ polarisation response of dielectric materials, specifically binary oxide dielectric materials, has been studied extensively as gate dielectric materials in TFTs with low voltage operation. Although having various superiority, metal oxide dielectric materials encounter some issues due to their lower bandgap, low band offset with existing metal oxides, a higher number of interfacial trap states owing to high polarity, and hygroscopic nature, which limits their use in reliable and stable device applications. In 2009, Pal et al. first time developed a sol-gel derived gate dielectric material (Sodium- β -Alumina, SBA) with higher ' κ ' value by introducing ionic doping into oxide lattices, and successfully employed as a gate insulator in low voltage TFTs. The higher ' κ ' value in SBA is generated because ionic

polarization that originated due to the Na ion movement in alumina matrix which facilitates operation of TFTs in low voltage regions. This ion-conducting metal oxide (ICMO) class of dielectric material essentially meets the requirement of moderate bandgap in addition to high- κ value. But, further studies on these SBA based TFT reveal that the hygroscopic nature of SBA or other alkali ions incorporated aluminas significantly degrade the device operations. This device property deterioration is attributed to the charge trapping at dielectric/semiconductor interface caused by rapid movement of alkali ions after physisorption of water molecules. So in concern of current challenges faced by high- κ ICMO dielectrics, I established some interfacial engineering with the ion-conducting dielectric material by a) using metal oxides semiconductor (like TiO_2 , Mn_2O_3) in between gate electrode and gate dielectric, and b) implementing a very smooth amorphous carbon (a-C) layer in between the gate dielectric and semiconductor layer to enhance the device performance. Furthermore, because of its tiny cell size, low power consumption, rapid write/erase speed, and nonvolatility, ferroelectric field effect transistor (FEFET) based memory storage is a viable alternative to flash and other existing nonvolatile memory technologies. Moreover, nondestructive read operation is the additional superiority of FEFETs over 1-transistor 2-capacitor (1T-2C) based memory technology. However, the reports on FEFET retention period are far from the ten-year retention standard for a non-volatile device, which is the main bottleneck in its widespread implementation. The two well studied reasons attributed to the shorter memory retention time are a) presence of the depolarization field and b) gate leakage current. Further, I have done some interfacial engineering with well established LiNbO_3 ferroelectric using ICMO to minimize depolarization field and leakage current. So, the main goal of my thesis work is to fabricate low operating voltage ICMO dielectric-based TFTs via a cost-effective solution process and improvement of the device performances in terms of threshold

voltage, subthreshold swing and current ON/OFF ratio through some interfacial engineering. Also, improvement of LiNbO₃ based FEFETs performances using ICMO dielectric as a charge compensating layer. As a whole, the thesis gives an outline of the use of ion-conducting materials as gate dielectrics and the intervening of different interface layers to form a bilayer or trilayer dielectric stack for the fabrication of high-performance and low-voltage TFTs. The thesis is arranged into seven chapters based on the aforementioned discussion:

Chapter 1 consists of a brief introduction of metal oxide thin-film transistors, its components and application along with the scope of my thesis work.

Chapter 2 discusses the material preparation of dielectrics, semiconductor, interfacial layer and thin film deposition through solution processed technique. Specifically in this thesis, the thin film of dielectric, semiconductor, and interfacial layers are deposited by spin coating method and used for TFT fabrication. In addition, the methodologies for characterization of materials and devices are thoroughly covered in this chapter.

The development of a high-performance sol-gel derived low operating voltage SnO₂ thin-film transistor with an ion-conduction Li-Al₂O₃ dielectric and a TiO₂ gate interface layer between the gate insulator and gate electrode is described in chapter 3. A comparative study of a set of SnO₂ TFTs with and without TiO₂ interface layer has been illustrated. The formation of a Schottky junction between p⁺⁺-Si and n-type TiO₂ aids in the accumulation of extra electrons at the Li-Al₂O₃/SnO₂ interface, which basically fills up the interface trap-states and diminishes the sub-threshold swing (SS) as well as threshold voltage (V_T) and increases the saturation carrier mobility of the device when compared to a device without TiO₂ interface. As contrasted to a bare Li-Al₂O₃ dielectric, the TiO₂/Li-Al₂O₃ stack dielectric with a high TiO₂ value improves

capacitance and lowers leakage current. In a $\text{TiO}_2/\text{Li-Al}_2\text{O}_3$ stack TFT with an ON/OFF ratio of 7.2×10^3 , it attained effective carrier mobility (μ) of $16.4 \text{ cm}^2 \cdot \text{V}^{-1} \cdot \text{s}^{-1}$, SS of $250 \text{ mV} \cdot \text{decade}^{-1}$, and V_T of 0.73 V . This research opens a new approach to developing high-performance TFT devices, using an appropriate bilayer stack of gate-dielectrics.

Chapter 4 depicts that the Mn_2O_3 gate interface can be used in between gate electrode and ionic gate dielectric to fabricate a high-performance solution-processed sub-volt tin oxide thin film transistor (TFT). A comparison of device characterization of two distinct TFTs with and without Mn_2O_3 gate interface reveals that Mn_2O_3 induces excess electrons to the semiconductor/dielectric interface trap states, lowering the device's threshold voltage and subthreshold swing. Furthermore, the depletion layer of the $\text{ITO}/\text{Mn}_2\text{O}_3$ interface suppresses gate leakage current, which helps to increase the device's ON/OFF ratio. A high capacitance of the dielectric film has been achieved by introducing a high- Mn_2O_3 layer between the $\text{Li-Al}_2\text{O}_3$ gate dielectric and the gate electrode. This helps in achieving current saturation at lower gate bias. The electron mobility of such a sub-volt TFT with an additional Mn_2O_3 layer in the gate dielectric is $17 \text{ cm}^2 \cdot \text{V}^{-1} \cdot \text{s}^{-1}$, the ON/OFF ratio is 3.3×10^4 , and the sub-threshold swing is $124 \text{ mV} \cdot \text{decade}^{-1}$. By identifying suitable material combinations for gate dielectrics, this study proposes a promising alternative approach for the development of high-performance, sub-volt TFT fabrication.

Chapter 5 illustrates a low-cost solution-processed LiNbO_3 based FEFET device fabrication and enhancement of its performances by introducing interfacial $\text{Li-Al}_2\text{O}_3$ dielectric material. The improved carrier mobility of $1.9 \text{ cm}^2 \cdot \text{V}^{-1} \cdot \text{s}^{-1}$, ON/OFF ratio of 1.6×10^4 and subthreshold swing of $167 \text{ mV} \cdot \text{decade}^{-1}$ are attained with $\text{Li-Al}_2\text{O}_3/\text{LiNbO}_3/\text{Li-Al}_2\text{O}_3$ stacked ferroelectric layer over only LiNbO_3 ferroelectric. The device also has a relatively long retention time. The improved performance of this device is explained by using a band model. It is proposed that the

intervening of the high bandgap Li-Al₂O₃ interfacial layer on both sides of LiNbO₃ results in complete charge compensation that originated due to ferroelectric polarization of LiNbO₃ thin film. In addition, this Li-Al₂O₃ interfacial layer prevents charge carrier injection from p⁺⁺-Si and SnO₂. These phenomena support the better operation of the FEFET device with Li-Al₂O₃/LiNbO₃/Li-Al₂O₃ stacked dielectric. This work demonstrates that the addition of an interfacial Li-Al₂O₃ layer significantly upgrades the electrical properties of the FEFET.

Chapter 6 deals with the comparative studies of two sets of SnO₂ thin film transistors with and without amorphous-carbon (a-C) semiconductor/dielectric interface layer using sol-gel-derived Li-Al₂O₃ as a gate dielectric. A remarkable change in the device performance has been realized by inserting a microwave synthesized ultra-smooth a-C layer between gate dielectric and semiconductor as a passivation layer. The coordination bond formation between N and Sn atoms helps for better growth of SnO₂ on the top of a-C layer. In addition, the high smoothness of the a-C layer essentially reduces the interface trap state densities by passivation of dangling bonds and defects of high- κ Li-Al₂O₃ dielectric. These phenomena effectively enhance the device performance and stability with a-C layer. Therefore, a better device performance has been achieved in terms of higher field effect mobility of 21.1 cm².V⁻¹.s⁻¹, ON/OFF ratio of 7.0×10⁴ and lower SS value of 147 mV.decade⁻¹ in the device with the a-C passivation layer. Also, this device exhibits lower hysteresis and better cyclic stability over the device without a-C layer. To the best of my knowledge, this is a very fast demonstration of the use of a-C layer as a semiconductor/dielectric interface modification layer to improve the metal oxide TFT device performance.

Finally, chapter 7 is devoted to summarizing the thesis's major findings. Lastly, the future scopes of work relevant to the current thesis have been sketched out briefly.

At the end of the thesis, there is a list of periodicals and books that were utilized to bind the thesis together as references.